DOI: 10.13009/EUCASS2019-322

Vortex Generators and Active Flow Control in the aft-deck of a Frigate

Juan Carlos Matías-García, Sebastian Nicolás Franchini-Longhi* and Rafael Bardera***
**Universidad Politécnica de Madrid (UPM), Madrid, Spain 28040*
jc.matias@alumnos.upm.es; s.franchini@upm.es
***Instituto Nacional de Técnica Aeroespacial (INTA), Torrejón de Ardoz, Madrid, 28850, Spain*
barderar@inta.es

Abstract

Aircraft are an essential tactical element and have great importance in all navies operations around the world. Their ability to combine their operations and provide support tasks to military frigates makes their operations near them very important. However, the pilot workload increases when the aircraft approaches the frigate. This is due to the airflow that surrounds the frigate is complex. High turbulence and low-velocity recirculation zones are typically present near them as a consequence of the non-aerodynamic design with sharp surfaces of the frigates. This makes helicopters or rotorcraft UAV's operations on frigates sometimes dangerous. Wind tunnel tests have been carried out to characterize and improve the flow on the aft-deck of a simplified frigate model (SFS2). In this area, where rotary-wing aircraft operate, the flow is typically affected by the presence of the frigate superstructure. Particle Image Velocimetry (PIV) has been used to obtain velocity maps at the aft-deck. Using these PIV maps, a parametric study of the flow and the recirculation bubble generated, that affects the aircraft performance on the deck, have been carried out. Passive control flow by trapezoidal vortex generators has been decided as a strategy for modifying the flow. The effects of changing their position have been analyzed. The suction or blowing power, and the position of the holes or grooves have been the parameters used for the active flow control characterization.

1. Introduction

Most of the military frigates have been designed for hosting helicopter operations on its aft-deck. This provides high flexibility in all the navy operations [1]. However, a frigate is composed of blunt bodies and its external surfaces are far from being aerodynamic. Due to this, the flow surrounding a frigate is very complex and it is characterized by detached flow with high-velocity gradients, direction changes and high turbulence intensity [2-3]. This means that helicopter pilots have to deal with low-frequency rotor oscillations and movements. Then, a greatly increasing of their workload during the landing approach to a frigate is produced, which increases the risk of an accident.

The non-aerodynamic shape of a frigate can be simplified and represented by a backward-facing-step that have been studied by some authors [4-5]. Other authors have presented more specific studies related to the frigate airwake and measurements of the flow above its flight deck. Some of them have been performed by numerical computation [6] and others by experimental data in wind tunnel testing [7-8] or on-board measurements [9]. The next step in the frigates aerodynamic studies has been performed taking into account the helicopter effect when it is flying near the frigate. Doane and Landman [10] performed wind tunnel tests of ship airwake and rotor coupling. Lee and Zan [11-12] carried out different wind tunnel tests to obtain the loads on a helicopter fuselage immersed in a ship airwake and helicopter rotor interaction with the ship airwake. Silva et al. performed Particle Image Velocimetry (PIV), force and moment measurements for determining the aerodynamic interaction between helicopters and tiltrotors during shipboard operations [13]. More PIV measurements near to a ship were recorded by Wadcock et al. [14] but this time using a tandem-rotor helicopter. For the numerical data, Wakefield et al. [15] made a CFD model to analyse the effect of having a hovering helicopter near ship structures under side winds and Foeken et al. [16] developed a model to reproduce helicopter flight operations near ships and the pilot issues during the landing approach.

Once discovered and analysed all the negative effects that the surrounding flow of a frigate can present for helicopters, investigations of airwake control for increasing helicopter safety during its operations have been carried out [17]. In this field, Shafer made an in-depth investigation publishing his Master Thesis about passive flow control over the flight deck of small naval vessels [18] and papers associated [19]. In general, flow control is a common research topic. A lot

DOI: 10.13009/EUCASS2019-322

of studies and papers have been published related to passive and active flow control in a wide variety of disciplines. Vortex generators are one of the most commons passive flow controllers. They generate vortex bringing energy to the flow to make it turbulent where necessary [20-22]. For example, they are useful to develop a turbulent boundary layer to delay the flow detachment [23-25]. Another way of flow control consists of active flow control devices [26]. Most typical active flow controllers are present in wing aerodynamics research and are based on suction [27] and blowing [28].

In the present paper, two different techniques of flow control in the aft-deck will be tested. Vortex generators over the hangar roof trying to energize the boundary layer and attach the flow to the frigate superstructure. Finally, active flow control using suction or blowing in order to reduce the size of the low-velocity region generated behind the superstructure and over the frigate helideck have been tested. All the results have been compared using velocity maps obtained by means of Particle Image Velocimetry (PIV).

2. Experimental set-up

2.1. Wind Tunnel and Particle Image Velocimetry (PIV)

All tests were performed at the wind tunnel test facilities of the National Institute of Aerospace Technology (INTA), in Spain. The wind tunnel T-1, is a low-velocity, closed circuit and open test section of $2\ m\ \times\ 3\ m$ wind tunnel. Using this tunnel, experimental tests up to 60 m/s with low turbulence intensity can be carried out. For obtaining velocity maps of the flow Particle Image Velocimetry (PIV) technique was used [29-33]. It is an advanced and non-intrusive velocity measurement technique which needs to seed the flow with small tracer particles such as atomized olive oil with particles around 1 μm used for these tests. The particles are illuminated by a powerful laser plane (ND: YAG) in order to capture their position by means of image pairs, separated a short period of time $\Delta t = 25\ \mu s$ using a digital camera with a 2048 x 2048 pixels CCD sensor. Then, by correlating each pair of images using *Fast Fourier Transform* (FFT) it is possible to obtain the cross-correlation peak in each small interest window selected of 32 x 32 pixels that indicates the average displacement of the particles in each one. With these displacements, a vector of displacement ($\Delta\vec{x}$) is known in each window. And as the time between the captures is known (Δt), the velocity on each window is also known ($\vec{v}$). In order to synchronise the laser pulse with the digital camera captures, a synchroniser model *Laser Pulse* 610035 was used. Laskin atomizers [34, 35] were used to generate the small tracer particles of atomized olive oil used for seeding the flow. Finally, *INSIGHT-3G* was the commercial software used for controlling the PIV equipment and correlate the image pairs. The resultant velocity maps were obtained averaging 100 pairs of captures and represented using *Tecplot360*.

2.2. Simplified Frigate Shape (SFS2)

The scaled frigate model (1:85) used for the test was a simplified frigate shape (SFS2), figure 1. It was a model proposed by NATO for frigate aerodynamic research [36-39]. In spite of its simplified geometry, it has the main components of a frigate: the bow at the front, the superstructure in the middle, the helicopter flight deck at the stern and the exhaust gases stack in the upper part. The SFS2 model used represents only the part of the frigate above the waterline. During the tests, the model was placed on a platform available on the wind tunnel test section which simulates the sea surface.

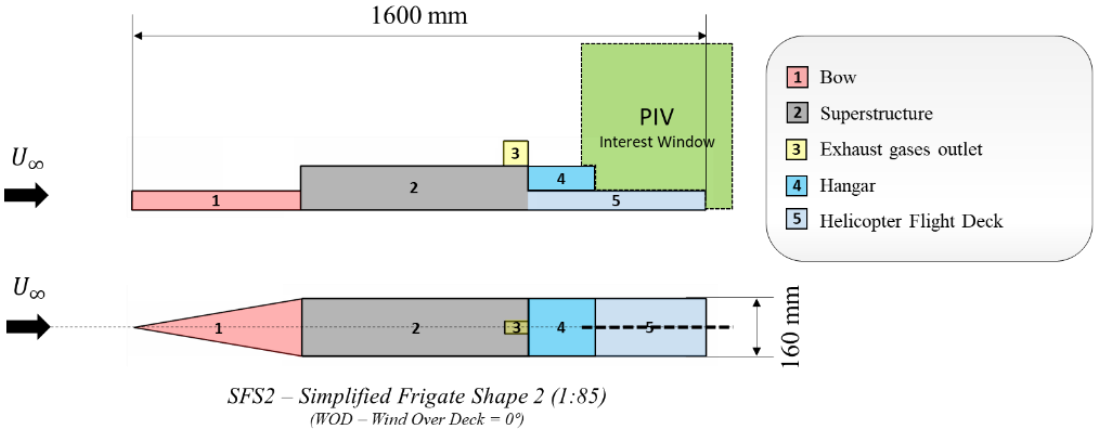

Figure 1: Simplified Frigate Shape 2 and interest region for PIV maps.

DOI: 10.13009/EUCASS2019-322

2.3. Passive Flow Control: Trapezoidal Vortex Generator

Vortex Generators [20-25] are passive flow control devices used for creating vortex downstream to an incident flow without any energy requirement, figure 2b. This vortex generation can be useful for energizing the boundary layer and make it turbulent. In this way, the boundary layer can better withstand adverse pressure gradients and delay their detachment. With a turbulent boundary layer, the flow can keep adhered to the surfaces in major changes of curvature. For creating this kind of vortex there are different shapes of vortex generators. One of the simplest is the Trapezoidal Vortex Generator (TVG), figure 2a. They consist on trapezoidal geometric shapes with gaps between them to generate the vortex behind them. The TVGs used for testing have been created by additive manufacturing using polylactic-acid (PLA) thermoplastic in a commercial 3D printer [40, 41]. Three different TVGs were printed with different angles to the horizontal plane, $\alpha = 0^o$, 30^o and 60^o, figure 2a. In figure 2d, TVGs placed on the roof corner of the frigate hangar are shown. For the tests they were placed at two different positions, hangar corner (a) and advanced to 1/3 of the hangar length (b) (TVGA), figure 2c. TVGs advanced from the hangar corner was tested in order to generate the vortex before and energize the boundary layer before the abrupt change in the geometry of the corner.

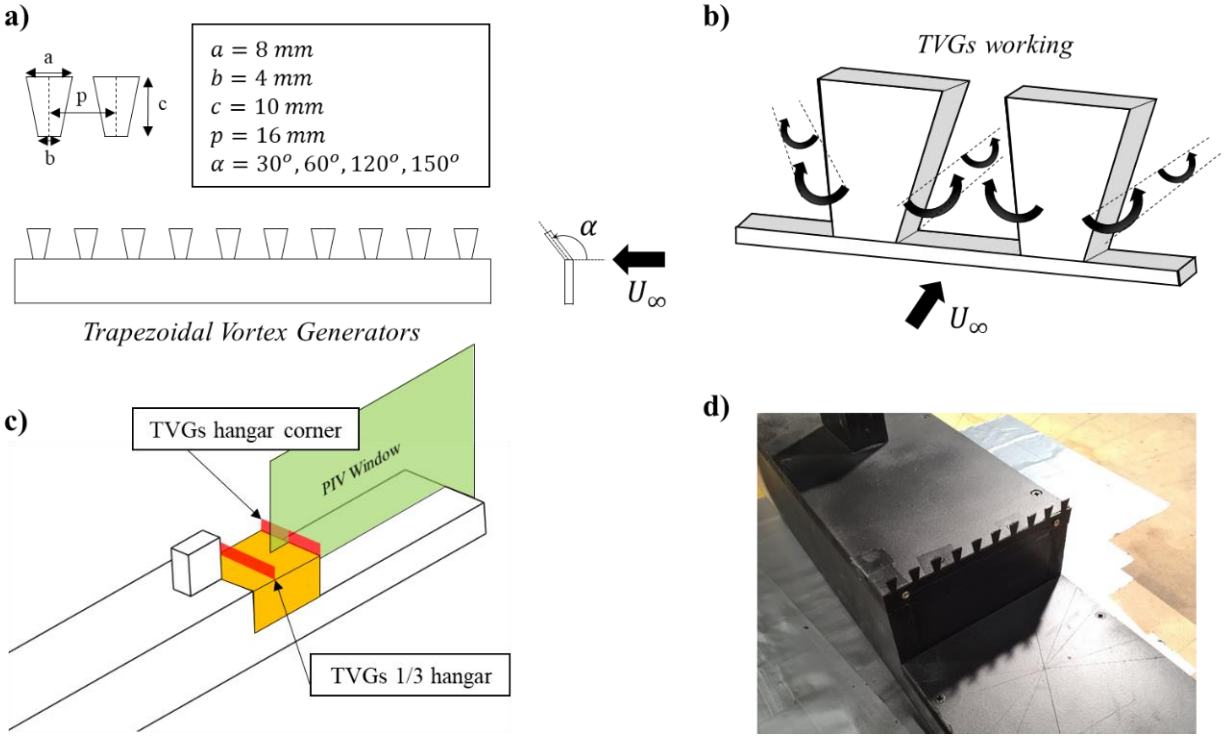

Figure 2: a) Trapezoidal Vortex Generators (TVGs) dimensions used for the tests. b) TVGs working and vortex creation behind them. c) Positions of the TVGs tested. d) TVGs placed on the SFS2 during wind tunnel testing.

2.4. Active Flow Control: Suction and Blowing

Suction and blowing near the hangar corner were the methods of active flow control tested for this study. For testing them, it was necessary to build a hermetically sealed hangar. Its structure was built in wood and fixed with screws. All internal joints were sealed using silicone. A tube was fixed at the bottom of the hangar to connect the suction and blowing air, figure 3a. A few drills near the hangar corner were made to allow the suction or blowing effect desired. These drills were made at the hangar roof (R), hangar side walls (W) and main hangar door (D), figure 3b and 3c. To produce the suction, a cyclonic vacuum system was used. It uses 2 kW when operating at full power, with a volume flow rate of 900 litres per minute. The blowing was produced by an industrial compressor with outlet pressure regulated by means of a threaded manometer. With this manometer, it was possible to adjust the outlet pressure between 2 and 4 bar. Using a Venturi tube, it was measured the total air flow rate used for each blowing case. Specifically, 816 l/min, 946 l/min, 1065 l/min and 1332 l/min for 2, 2.5, 3 and 4 bar cases, respectively.

DOI: 10.13009/EUCASS2019-322

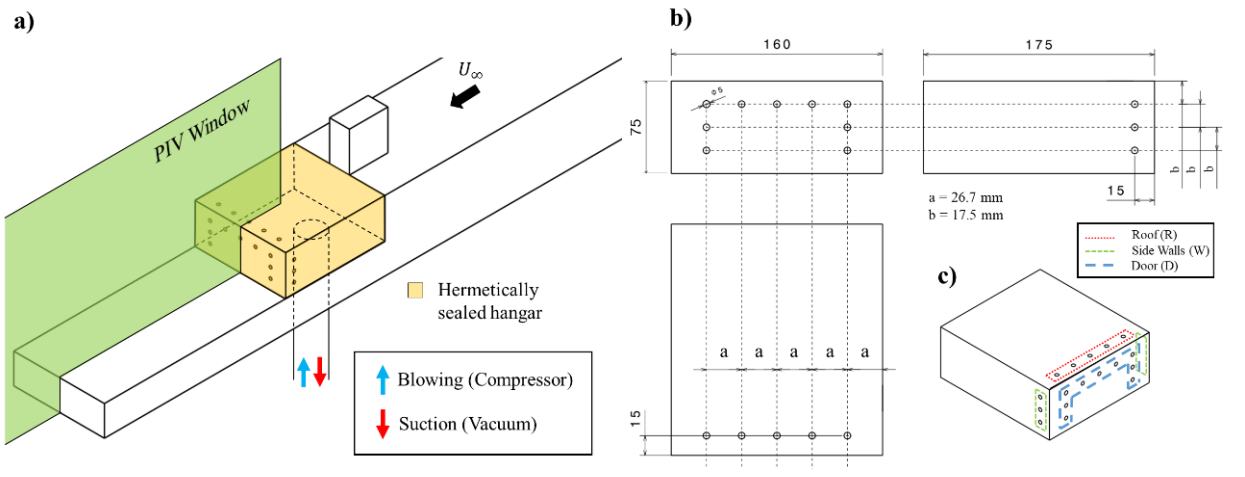

Figure 3: a) Hermetically sealed hangar on the SFS2 model and suction/blowing tube for testing. b) Arrangement of the drills in the hangar and named holes.

Figure 4 shows three photographs during wind tunnel test experiments. Figure 4a shows a TVG $\alpha = 150^o$ placed at 1/3 of the hangar roof length. Figure 4b presents a smoke visualization test to check the suction working using the sealed hangar. Finally, *figure 4c* shows the SFS2 model placed at the test section of the wind tunnel.

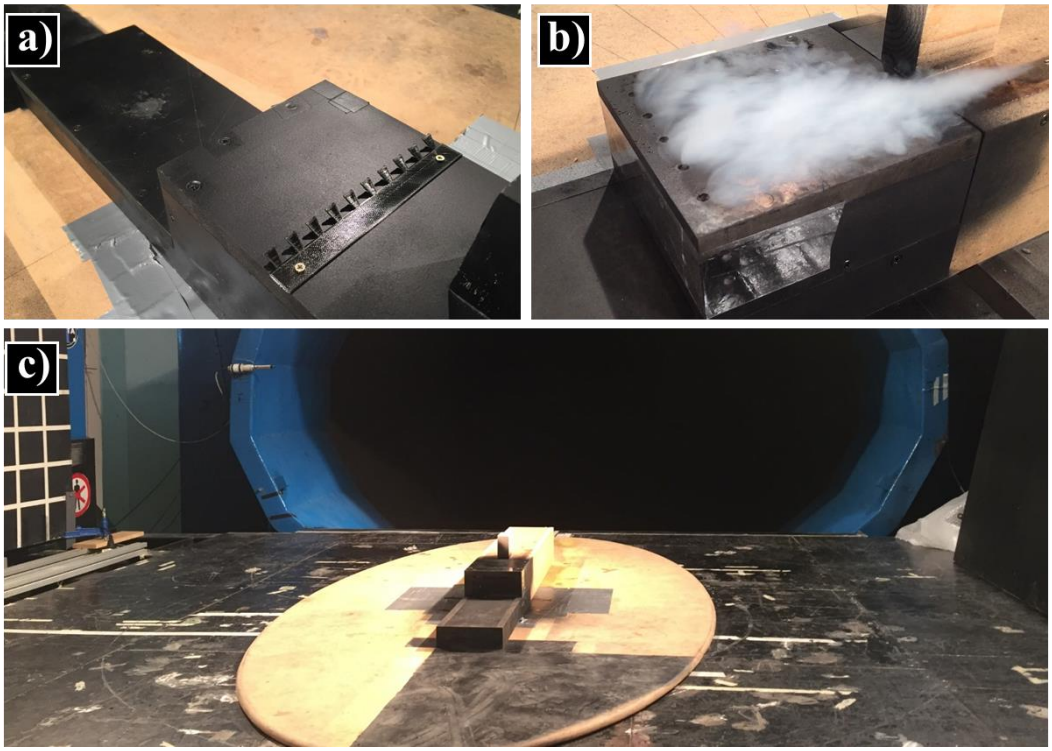

Figure 4: a) TVG 150º during tests. b) Visualization smoke test to check the proper suction of the sealed hangar before PIV testing. c) SFS2 model at the wind tunnel test section during active flow control testing.

3. Results

3.1. Base flow

Non-dimensional velocity map over the aft-deck of the frigate without any flow control device is shown in figure 5a. It presents a big low-velocity region with a recirculation bubble inside it. This region is created due to flow detachment

DOI: 10.13009/EUCASS2019-322

in the descending step that the frigate superstructure forms with the helicopter flight deck. The main flow patterns of the flow above the frigate flight deck at the stern is presented in the simplified scheme of the figure 5c. From the top to the bottom, FS is the free-stream velocity without any frigate influence, SL-1 and LSR are the first shear layer and the low-speed region produced by the frigate aerodynamic interference upstream. Finally, a second shear layer appears (SL-2) with a big recirculation bubble (RB-1) underneath due to the flow detachment at the end of the frigate superstructure. Another shear layer and its corresponding recirculation bubble appears just behind the frigate flight deck and over the sea (SL-3, RB-2). Figure 5b contains a table with data extracted from the recirculation bubble. Bubble size (height and width), and its centre measured from the helicopter landing spot over the flight deck ($x = 0\ mm, y = 0\ mm$) for test modelling scale (1:85th) and full-scale case are displayed.

In view of results, UAV's or helicopter rotor performance could be affected by this low-velocity region and the recirculation bubble presented during the landing approach. It can suffer oscillations and low-frequency movements that increase the pilot workload during the manoeuvre.

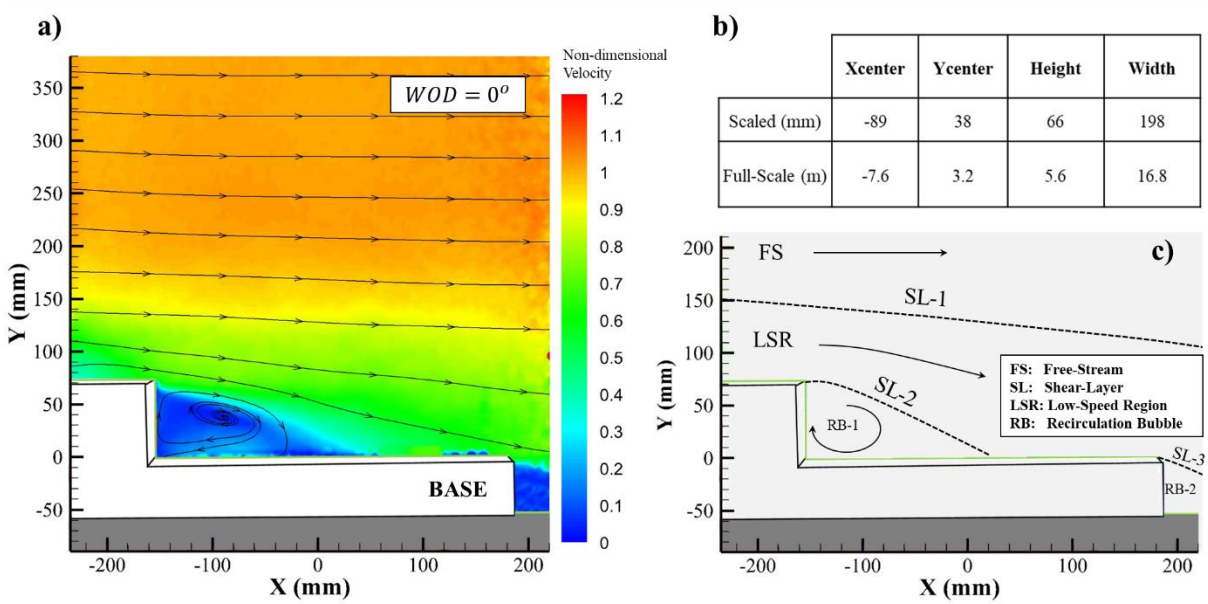

	Xcenter	Ycenter	Height	Width
Scaled (mm)	-89	38	66	198
Full-Scale (m)	-7.6	3.2	5.6	16.8

Figure 5: a) Base configuration non-dimensional velocity map at Wind Over Deck of 0º. b) Characteristics of the low-velocity region and recirculation bubble generated. Coordinates measured from the helicopter landing spot (0 mm, 0 mm). c) Schematic representation of the flow patterns.

3.2. Passive and Active Flow Control: Non-dimensional Velocity maps

The results of non-dimensional velocity maps above the flight deck using trapezoidal vortex generators (TVGs) are shown in figures 6 and 7. Figure 6 presents the results of the actuators placed right over the corner of the hangar and the comparison maps through their difference with the base case. Figure 7 shows the results and difference maps with the base case when the actuators are placed upstream, at 1/3 the length of the hangar (TVGAs). All difference maps presents the subtraction of non-dimensional velocities (V^*) between the case study and the base flow showed on *figure 5a*. Then, looking to the difference maps presented using TVGs, there is a growth in the height of the recirculation bubble, with velocity decrease up to 40 % on this region (red tones on difference maps). There is also no improvement observed in the reduction of its size and extension above the helideck. Therefore, using TVGs in the hangar corner does not present any advantage over the base case. The following case of advanced TVGs (TVGsA) has better results in terms of the smaller height of the low-velocity region. It may be because the boundary layer that now has more energy injected through the vortex generated tries to attach to the geometry in the hangar corner. However, the turn that the flow has to make there is very abrupt and the flow ends up detaching again in a similar way than the base case. In addition, the difference maps show again a slightly velocity decrease of 8 % using TVGAs (yellow tones on difference maps) of the flow over the flight deck whose effect is not positive for the helicopter rotor performance. To sum up, the results of these TVGs advanced are similar to the base case. It is possible to anticipate that this type of vortex generators can work well in softer geometries. However, using them it is impossible to avoid the detachment of the flow in descending steps as it is the final part of the frigate superstructure.

DOI: 10.13009/EUCASS2019-322

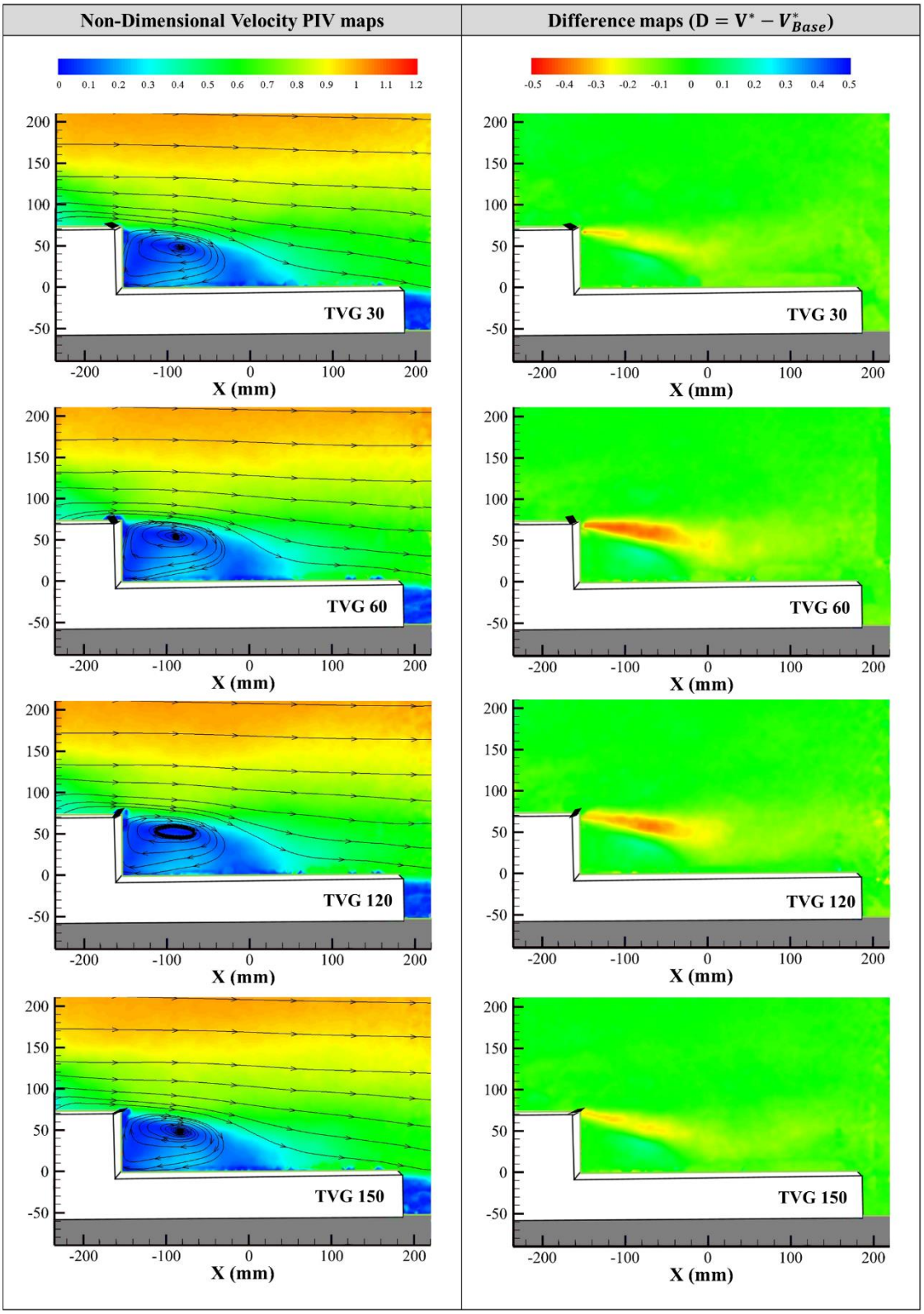

Figure 6: Non-Dimensional velocity maps of Trapezoidal Vortex Generators (TVGs) tested at the hangar corner. Number represents the angle (α) of the device against the incident flow

DOI: 10.13009/EUCASS2019-322

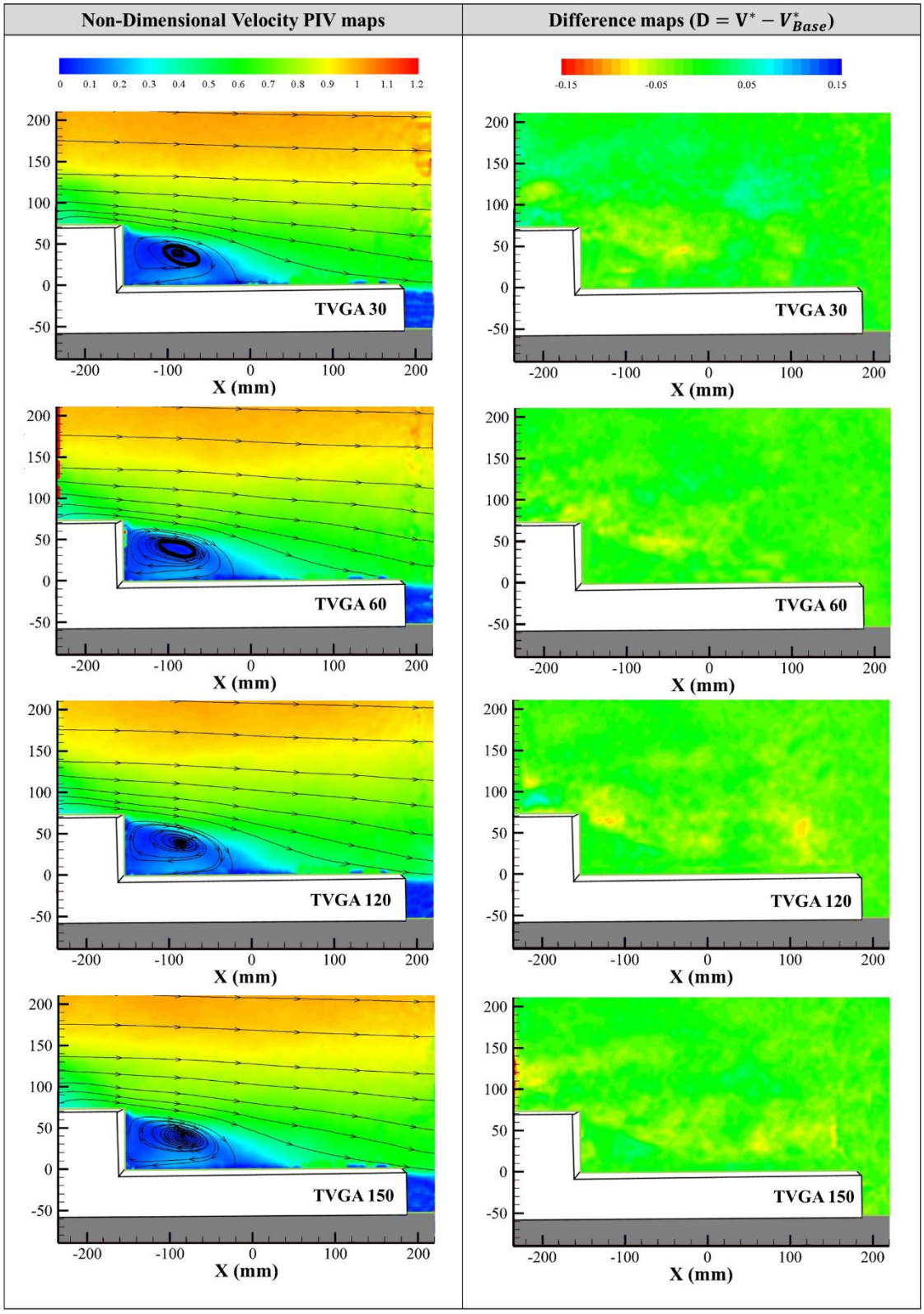

Figure 7: Non-Dimensional velocity maps of vortex generators tested at an advanced distance 1/3 of the hangar length (TVGAs). Number represents the angle (α) of the device against the incident flow.

DOI: 10.13009/EUCASS2019-322

Active flow control was tested by means of suction and blowing. The resultant velocity maps applying suction to the hangar corner are presented in figure 8. The four maps present different ways of suction tested. First and second maps correspond to suction only from the holes of the door (D) and the hangar roof (R). Results with combined suction from the roof and side walls (R + W) and from all holes (D + R + W) are showed in third and fourth maps.

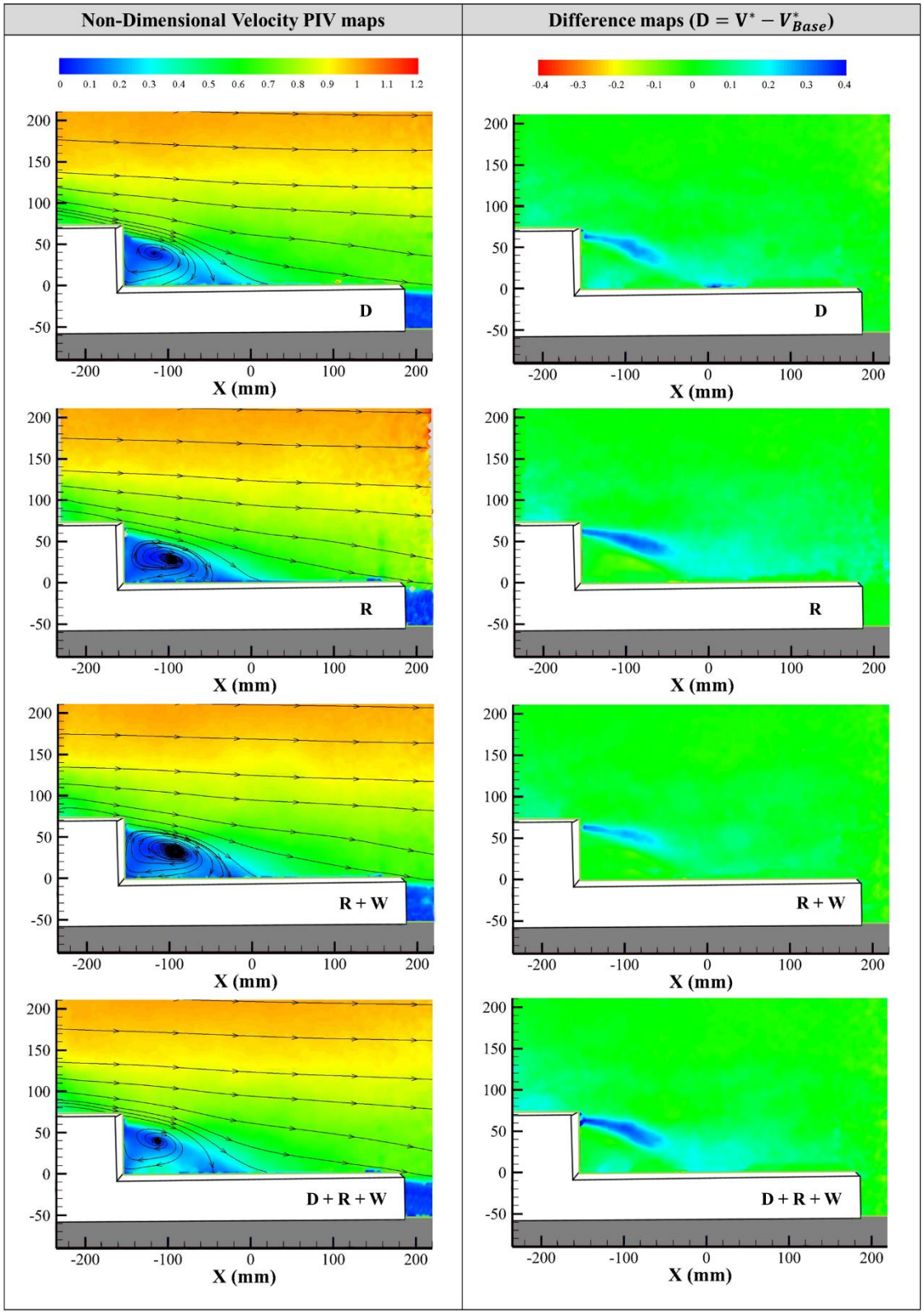

Figure 8: Non-Dimensional Velocity maps of active flow control using suction at hangar main door (D), roof (R) and side wall (W).

DOI: 10.13009/EUCASS2019-322

Looking into difference maps against the base case, it is clear that the fully-combined suction (D+R+W), and single suction cases of door (D) and roof (R) are the ones that achieve the best results. The low-velocity region has been reduced in its upper part (blue region of the difference maps), due to a velocity increase around 40 % at this region. The last case tested of using blowing was performed using different pressure outlet values (and therefore different blowing speeds) of the compressor used for achieving this blowing effect, figure 9.

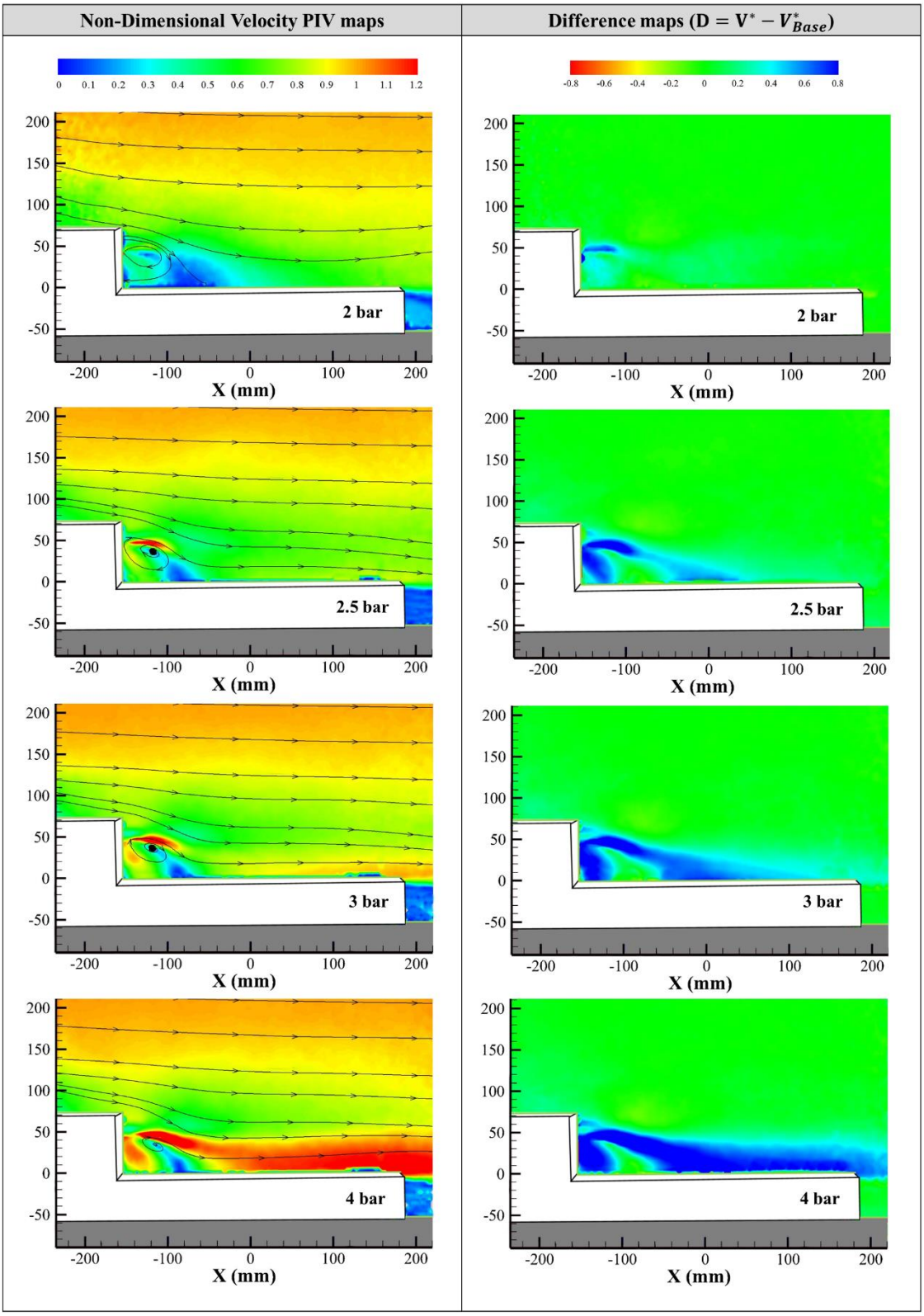

Figure 9: Non-Dimensional Velocity maps of active flow control using blowing from the hangar door.

DOI: 10.13009/EUCASS2019-322

All cases of blowing were made blowing only from the holes of the door (D). This was selected because blowing from the side walls (W) or hangar roof (R) would increase the flow detachment from the hangar corner. From the velocity maps, it is easy to observe that recirculation bubble is not fully deleted but the major area of the low-velocity region has disappeared, except the first case tested with air pressure of 2 bars (816 l/min). From the difference maps, the first case (2 bar) presents a flow acceleration right at the blowing injecting zone. However, it is not enough to eliminate the low-speed zone. All other cases present a greater velocity at the injection zone (higher when the pressure outlet increases) and they get to replace the low-speed zone by a zone with speeds equal to the current above the shear layer (SL-2, figure 5c) of the bubble (2.5 bar, 946 l/min) or even higher (3 and 4 bar, 1065 l/min and 1332 l/min, respectively). Cases with pressures of less than 2 bars were tested without any promising results.

4. Detailed comparison of the results

In order to quantify the different cases tested, a more detailed comparison were made. This comparison was focused on the size of the low-velocity region above the frigate flight deck and the velocity profile that a helicopter rotor would find during the landing approach. During this landing approach, the rotor is usually working at 5 meters of height above the deck (58 mm in the 1:85th scaled case). For comparing the area occupied by the low-velocity region, a Low-Speed Area above the flight-deck parameter (LSA) is defined, figure 10. In terms of velocity, the bubble area (A_B) is defined as the region of the flow with non-dimensional velocity (V^*) under 0.3 value. For plotting the velocity profiles on the helicopter rotor, 86 data points from PIV maps were used for each case on the rotor line ($y = 58$ mm), figure 10.

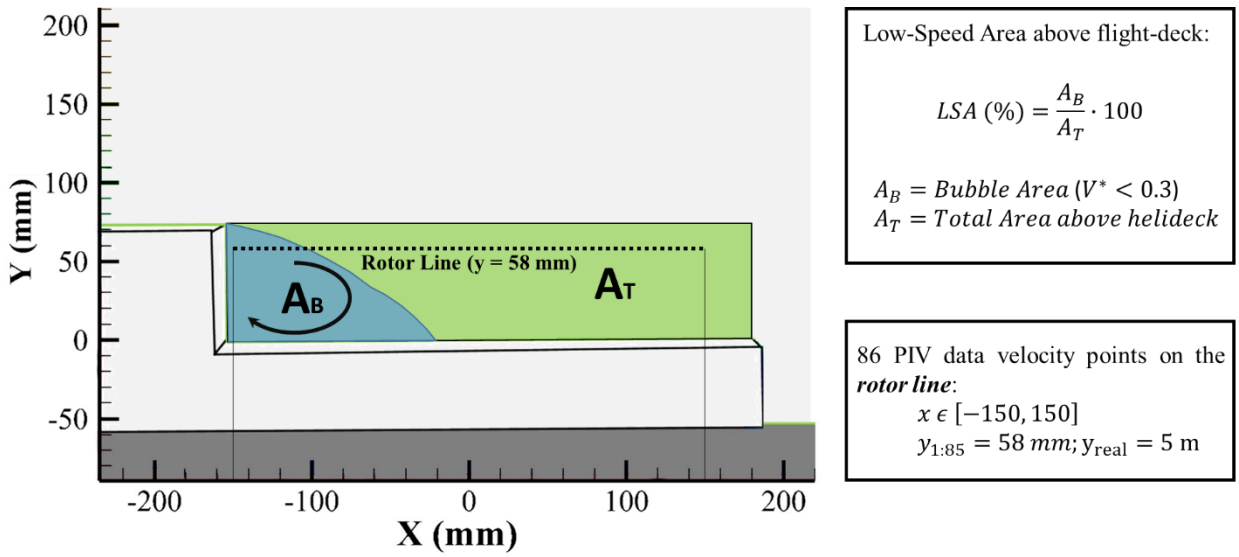

Figure 10: Graphical scheme for comparative analysis: definition of bubble and total helideck areas, Low-Speed Area proportion over the flight-deck (LSA) and the rotor line.

This way, the proportion of the low-speed area above the flight-deck (LSA) can be compared for all cases in figure 11 and the velocity profiles on the rotor line in figure 12. LSA parameter values show that passive flow controllers did not achieve encouraging results. The size of the recirculation bubble increased an average of 13 % for the TVGs and 2 % for TVGs advanced compared to the base flow (LSA = 36 %). Better results were obtained with active flow control. Single suction from hangar door (D) and roof (R) reduce Low-Speed Area (LSA) of 23 and 25 %, respectively. Combined suction from the roof and side walls of the hangar (R + W) reduces a 7 % of the low-velocity area relative to the base configuration. The best results were obtained with the total combined suction (D + R + W), with a resultant low-velocity area reduction of 14 % (LSA = 22 %).

Finally, even better results were achieved using blowing from the door holes (D). In all cases, there was a reduction in the low-velocity area. The case with the lowest blowing power (2 bar) achieved a reduction of 15 % of that area. All other cases present an average reduction of almost 30 % with regard to the base case. There was almost no difference between these last three cases. Using 2.5 bar of the outlet pressure at the compressor used for blowing tests, an LSA of 8.4 % was achieved. And for the higher cases of 3 and 4 bar, despite enormously accelerating the flow, they achieved a little less LSA parameter of 7.3 and 6.8 %. For that reason, the large increase in power involved in generating that blow increment on the full-scale case could not compensate for the benefits and would be enough with the case of 2.5 bars.

DOI: 10.13009/EUCASS2019-322

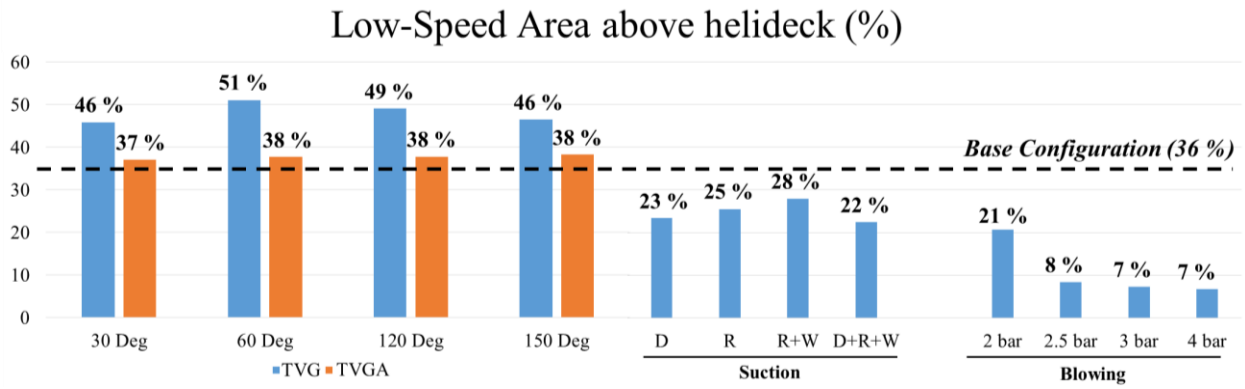

Figure 11: Low-speed areas above helideck - LSA (%) of the different configurations tested.

Figure 12 shows the non-dimensional velocity profiles on the helicopter rotor line. They show more or less the same trends than in the LSA parameter from the previous part of the comparison. The passive flow devices (TVGs) produced a velocity decrease at the nearest points of the helicopter rotor to the frigate superstructure, from $x = -150$ mm to $x = -50$ mm, that is a negative effect for helicopter operation. Advanced TVGs did not produce any visible effect on the rotor velocity profiles. On the contrary, active flow control improved the velocity profiles increasing the velocity value on this side of the profile. Using suction, the mean velocity over the flight deck ($V_{adim} \sim 0.75$) was achieved around 50 mm before than the base case, at $x = -100$ mm. Finally, using blowing, the velocity profiles on the rotor were almost constant over the full flight deck, which is better for reducing oscillations and low-frequency movements.

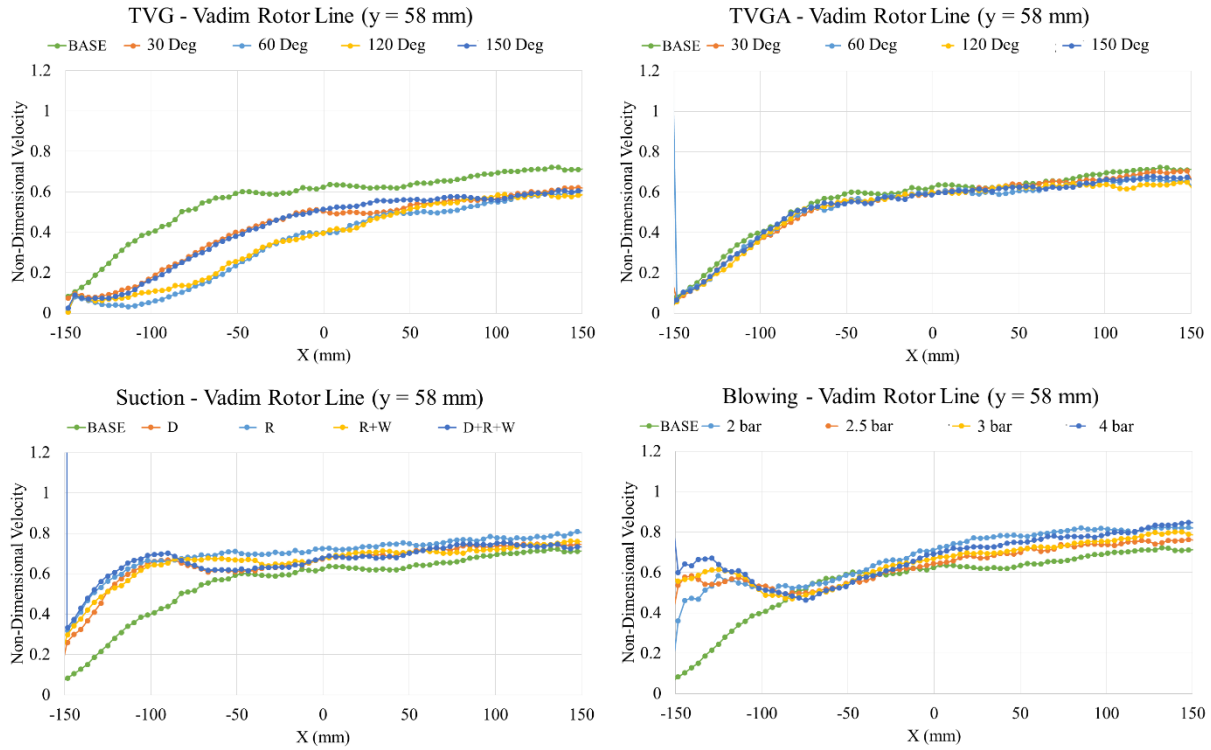

Figure 12: Non-dimensional velocity profiles on the rotor line for all cases tested against base configuration.

5. Conclusions

In this paper, the flow over the helicopter flight deck of a simplified frigate shape has been studied by means of Particle Image Velocimetry (PIV) on wind tunnel tests. From the velocity maps extracted from tests, the base flow has been analyzed finding the aerodynamic problems that a helicopter can expect during its landing approach on frigates. Different shear layers, low-velocity regions and recirculation bubbles appear just behind the frigate superstructure. That leads to generate oscillations and low-frequency movements for the helicopter or UAV's rotor that can increase

DOI: 10.13009/EUCASS2019-322

the pilot workload during the maneuver. For that reason, several attempts to reduce the low-velocity region size have been tested. On one hand, passive flow controllers have been tested using trapezoidal vortex generators placed over the roof hangar. Results with these devices have shown that the low-velocity region increases its size or remains the same as the reference base case. Therefore, no improvement has been found using these devices on the hangar. On the other hand, active flow control has been tested using suction and blowing near the hangar corner in order to reduce the recirculation bubble size and balance incident velocities to the helicopter rotor (rotor line velocity profiles). Suction over different faces of the hangar (door, roof and side walls) have achieved a decrease of 14 % of low-velocity region area and blowing from the hangar door up to 28 %. Rotor incident velocity profiles have also been improved using these flow control techniques. These improvements can lead to an increase in the safety of future helicopters operations on frigates. However, this study is a first approach conceptual step to introduce active flow control in the aft-deck of a frigate. More detailed research studies will be necessary to quantify the energy cost required for these ways of controlling the flow in the full-scale case and to see if it is viable and practical for the real frigates case.

References

[1] Kääriä, C., Y. Wang, M. White and I. Owen. 2013. An experimental technique for evaluating the aerodynamic impact of ship superstructures on helicopter operations. *Ocean Engineering*. 61:97-108.

[2] Healey, J. V. 1992. Establishing a database for flight in the wakes of structures. *Journal of Aircraft*. 29(4):559-564. Journal of the American Helicopter Society

[3] Kääriä, C. 2012. Investigating the impact of ship superstructure aerodynamics on maritime helicopter operations. PhD Thesis. School of Engineering. University of Liverpool, UK.

[4] Nacakli, Y., D. Landman and S. Doane. 2012. Investigation of Backward-Facing-Step Flow Field for Dynamic Interface Application. *Journal of the American Helicopter Society* 57(3):1-9.

[5] Rajasekaran, J. 2011. On the flow characteristics behind a backward-facing step and the design of a new axisymmetric model for their study. PhD Thesis, University of Toronto.

[6] Polsky, S. 2003. CFD prediction of airwake flowfields for ships experiencing beam winds. In : *21st AIAA Applied Aerodynamics Conference*. 3657.

[7] Swales, C. and G. Breeze. 1997. LDV measurements above the flight deck of a model frigate. In: *35th aerospace sciences meeting & exhibit*, Reno, NV, 6-9. Reston, VA: AIAA.

[8] Bardera-Mora, R., M. Barcala-Montejano, A. Rodríguez-Sevillano, G. de Diego and M. de Sotto. 2015. A spectral analysis of laser Doppler anemometry turbulent flow measurements in a ship air wake, *Proceedings of the Institution of Mechanical Engineers, Part G: Journal of Aerospace Engineering*. 229 (12): 2309-2320.

[9] Brownell, C., L. Luznik, M. Snyder, H. Kang and C. Wilkinson. 2012. In Situ Velocity Measurements in the Near-Wake of a Ship Superstructure, *Journal of Aircraft*. 49(5):1440-1450.

[10] Doane, S. R. and D.A. Landman. 2012. A wind tunnel investigation of ship airwake/rotor downwash coupling using design of experiments methologies. In: *Proceedings of the 50th AIAA Aerospace Sciences Meeting including the New Horizons Forum and Aerospace Exposition*. 2012-0767.

[11] Lee, R. and S. Zan. 2002. Wind tunnel testing to determine unsteady loads on a helicopter fuselage in a ship airwake. In : *ICAS 2002 Congress*. 3111-1

[12] Lee, R. and S. Zan. 2005. Wind Tunnel Testing of a Helicopter Fuselage and Rotor in a Ship Airwake. *Journal of the American Helicopter Society*. 50(4):326-337.

[13] Silva, M. J., G. K. Yamauchi, A. J. Wadcock and K. R. Long. 2004. Wind tunnel investigation of the aerodynamic interactions between helicopters and tiltrotors in a shipboard environment. *Naval air systems command Patuxent river MD*.

[14] Wadcock, A. J., G. K. Yamauchi, J. T. Heineck, M. J. Silva and K. R. Long. 2004. PIV Measurements of the Wake of a Tandem-Rotor Helicopter in Proximity to a Ship. *National Aeronautics and space administration moffett field CA AMES research center*.

DOI: 10.13009/EUCASS2019-322

[15] Wakefield, N., S. Newman and P. Wilson P. 2002. Helicopter flight around a ship's' superstructure. *Proceedings of the Institution of Mechanical Engineers, Part G: Journal of Aerospace Engineering*. 216(1): 13-28.

[16] Foeken, M., M. D. Pavel. Investigation on the simulation of helicopter/ship operations. F*aculty of Aerospace Engineering, Delft University of Technology* Kluyverweg 1, 2629 HS, Delft, The Netherlands.

[17] Lumsden, R. B. 2003. Ship air-wake measurement, prediction, modelling and mitigation Defence Science and Technology Laboratory, UK.

[18] Shafer, D. M. Active and passive flow control over the flight deck of small naval vessels. PhD Thesis. Faculty of the Virginia Polytechnic Institute and State University.

[19] Shafer, D.M., T. A. Ghee. 2005. Active and passive flow control over the flight deck of small naval vessels. In : *35th AIAA Fluid Dynamics conference and Exhibit, Fluid Dynamics and Colocated Conferences*, Toronto, Ontario, Canada.

[20] Aider, JL., JF Beaudoin and Wesfreid, J.E. 2010. Drag and lift reduction of a 3D bluff-body using active vortex generators. *Exp Fluids* 48: 771.

[21] Betterton J.G., H.C. Hackett, P.R. Ashill, M.J. Wilson, I.J. Woodcock, C.P. Tilman, K.J. Langan KJ. 2000. Laser doppler anemometry investigation on sub boundary layer vortex generators for flow control. In: P*roceeding of the 10th symposium on application of laser techniques to fluid mechanics*. Lisbon, Portugal

[22] Smith F. T. 1994. Theoretical prediction and design for vortex generators in turbulent boundary layers. *J Fluid Mech* 270:91–131

[23] Duriez T, J-L Aider, JE Wesfreid. 2006. Base flow modication by streamwise vortices. Application to the control of separated flows. In : *Control of Separated Flows*, ASME technical paper FEDSM2006-98541. Miami, USA

[24] Duriez T, Aider J-L, Wesfreid JE. 2008. Linear modulation of a boundary layer induced by vortex generators. In: *4th Flow control conference, AIAA technical paper* AIAA-2008-4076. Seattle, USA.

[25] Lin J. 2002. Review of research on low-profile vortex generators to control boundary-layer separation. Prog Aerosp Sci 38:389–420

[26] Oktay, T. and O. Kanat. 2017. A Review of Aerodynamic Active Flow Control. In: *IATS 2017*, Turkey.

[27] Kianoosh Y., S. Reza. 2015. Three-dimensional suction flow control and suction jet length optimization of NACA 0012 wing. Meccanica, Springer Verlag, 50 (6), pp.1481-1494. 10.1007/s11012015-0100-9. hal-01590679

[28] S Baljit, S, M. Saad, A. Z Nasib, A. Sani, R. Mohd and R. Abdul, Azam. 2017. Suction and Blowing Flow Control on Airfoil for Drag Reduction in Subsonic Flow. *Journal of Physics: Conference Series*. 914. 012009. 10.1088/1742-6596/914/1/012009

[29] Adrian, R. and J. Westerweel. 2011. Particle Image Velocimetry. *Cambridge: Cambridge University Press.*

[30] Adrian, R. J. 1991. Particle-imaging techniques for experimental fluid mechanics. *Annual review of fluid mechanics*, 23(1), 261-304.

[31] Adrian, R. J., & Westerweel, J. 2011. Particle image velocimetry (No. 30). Cambridge University Press.

[32] Prasad, A. K. 2000. Particle image velocimetry. CURRENT SCIENCE-BANGALORE-, 79(1), 51-60.

[33] Raffel, M. C. Willert, F. Scarano, C. Kähler, S. Wereley and J. Kompenhans. 2007. Particle Image Velocimetry. Springer.

[34] Echols, W. H. and J. A. Young. 1963. Studies of portable air-operated aerosol generators (No. NRL-5929). NAVAL RESEARCH LAB WASHINGTON DC.

[35] Kähler, C., B. Sammler and J. Kompenhans. 2002. Generation and control of tracer particles for optical flow investigations in air, *Experiments in Fluids*. 33(6):736-742.

DOI: 10.13009/EUCASS2019-322

[36] S. J. Zan. 2000. Surface Flow Topology for a Simple Frigate Shape. *Canadian Aeronautics and Space Journal. 47:33-43*

[37] Bardera, R. 2014. Experimental Investigation of the Flow on a Simple Frigate Shape (SFS). *The Scientific World Journal*, 2014:1-8.

[38] Yuan W., R. Lee and A. Wall 2016. Simulation of Unsteady Ship Airwakes Using Openfoam. In : *30th Congress of the International Council of the Aeronautical Sciences*. DCC, Daejeon, Korea: September 25-30.

[39] Yuan, W., A. Wall and R. Lee. 2018. Combined numerical and experimental simulations of unsteady ship airwakes. *Computers & Fluids*, 172: 29-53.

[40] Springer, A. 1998. Evaluating aerodynamic characteristics of wind-tunnel models produced by rapid prototyping methods. *Journal of Spacecraft and rockets*, 35 (6):755-759.

[41] Tyler, C., W. Braisted and J. Higgins, J. 2005. Evaluation of rapid prototyping technologiesfor use in wind tunnel model fabrication. In: *43rd AIAA Aerospace Sciences Meeting and Exhibit*, Reno, NV, AIAA 1301:10-13.